Concentration Profile of Polymer Solutions near a Solid Wall

D. Ausserré, H. Hervet, and F. Rondelez
Physique de la Matière Condensée, Collège de France, F-75231 Paris Cedex 05, France
(Received 7 January 1985)

Application of the evanescent-wave-induced fluorescence technique to the study of the interfacial depletion layer between a polymer solution and a solid barrier has yielded the first measurement of the monomer concentration as a function of the distance to the wall. The results have been obtained on a dilute aqueous solution of xanthan, a stiff polysaccharide of high molecular weight. The data are described quantitatively by an empirical model for semiflexible chains. Good agreement is also found with the Auvray model for fully rigid rods, for an equivalent rod length of $L = 600 \pm 10$ nm.

PACS numbers: 68.45.–v, 36.20.Ey

The repulsion exerted by a solid, impenetrable, wall on macromolecular chains in solution is a simple conceptual problem. It has been shown first by Asakura and Oosawa[1] that, even in the absence of specific interactions between the wall and the solute, the chains experience a repulsive entropic force, due to the excluded-volume effect, every time they try to approach the wall closer than a certain characteristic distance. The detailed monomer concentration profile $\Phi(Z)$ for dilute polymer solutions has been worked out by a variety of theortical tools. Monte Carlo simulations,[2] mean-field methods,[3,4] random-flight statistics,[5] and scaling arguments[6,7] have been used successively in the case of flexible coils. The concentration profile in the rigid-rod case has been constructed by Auvray using considerations on the configurational entropy.[8]

The experimental situation is, however, much less resolved. If we except indirect rheological data in fine pores,[9] the detection of the minute polymer concentrations involved in the interfacial depletion layers has so far eluded the skill of the experimentalists. On the other hand, there has been a growing recognition that depletion layers do play a role in a number of potentially important processes for the stabilization-destabilization of colloidal systems by polymeric additives.[10]

In an earlier report, we have shown how the optical evanescent waves which set in, under certain conditions, at the boundary between two transparent media of different refractive indexes can be used to probe the interface between a solid and a polymer solution over submicroscopic distances.[11] At that time, however, the results had been limited to the determination of the overall thickness range in which the solute concentration was affected by the wall. Technical improvements, plus the choice of a polymer chain with an end-to-end distance comparable to the penetration depth of the evanescent wave, now allow us to present the first quantitative observation of the density profile for solutions of stiff polymers in the repulsive case. The results in dilute solutions are in agreement with the theoretical models when the local chain rigidity is taken into account.

Aqueous solutions (0.1M NaCl, 400 ppm NaN_3) of xanthan covalently labeled with fluorescein chromophores (1% of the monomers labeled) were obtained from the Institut Francais du Pétrole and used at a fixed concentration of 96×10^{-6} g/g. Solutions were filtered through a 2-μm Nucleopore membrane before use to eliminate small aggregates. The average molecular weight M_w was 1.8×10^6 and the polydispersity $M_w/M_n = 1.35$. This particular batch has been fully characterized by viscometry and light scattering following fractionation by surface-exclusion chromatography.[12] The molecule can be modeled as a semiflexible monohelical rod of persistence length $q = 50 \pm 2$ nm and molecular diameter $d = 1.9$ nm.[13] With a linear mass density taken as $M_L = 10^3$ u/nm, its contour length is calculated to be $L_c = 1.8$ μm. From the Kratky-Porod formula from wormlike chains,[14] we estimate its end-to-end distance to be $L = 420$ nm. This value is much larger than the 60-nm value corresponding to the random-coil conformation with bond-angle rotation restriction.[15] This mere fact puts the expected depletion-layer thickness well into the range accessible to optical evanescent waves.

The experimental setup has been described extensively elsewhere.[16] A collimated light beam (wavelength $\lambda_0 = 488$ nm) propagating in a medium of high refractive index (fused silica, $n_1 = 1.436$) and impinging on a flat interface with a medium of low refractive index (aqueous polymer solution, $n_2 \simeq 1.334$) experiences total reflection for all angles θ larger than a critical angle $\theta_c = \sin^{-1}(n_2/n_1)$. An exponentially decaying intensity nevertheless penetrates the rarer medium over a characteristic length

$$\Lambda = \lambda_0(4\pi n_1)^{-1}(\sin^2\theta - \sin^2\theta_c)^{-1/2}.$$

Adjusting θ between θ_c and $\pi/2$ allows one to tune Λ from ∞ down to 70 nm. This evanescent wave is used to excite the fluorescence of the polymer solution. The detected intensity, $I_F^{pol}(\Lambda)$, is the integrated product of the evanescent wave energy with $\Phi'(Z)$, the chro-

© 1985 The American Physical Society

mophore concentration profile. For a random distribution of chromophores along the chain, it is reasonable to assume that $\Phi(Z)$ will be proportional to $\Phi'(Z)$. Therefore

$$I_F^{\rm pol}(\Lambda) \propto \int_0^\infty \Phi(Z)\exp(-Z/\Lambda)\,dZ.$$

All prefactors can be neglected here since they cancel out when we take the ratio between $I_F^{\rm pol}(\Lambda)$ and the fluorescence intensity $I_F^{\rm ref}(\Lambda)$ emitted by a reference solution composed of unlabeled polymer and free fluorescein chromophores at the same bulk concentration Φ_b. It is then possible to write $R(\Lambda)$ as an equality such that

$$R(\Lambda) = \frac{I_F^{\rm pol}}{I_F^{\rm ref}} = \frac{1}{\Phi_b \Lambda}\int_0^\infty \Phi(Z)\exp\left(-\frac{Z}{\Lambda}\right)dZ. \quad (1)$$

The polymer solution was contained between the dugout part of a separable flow-through Hellma cuvette and the top surface of a fused silica prism. Fused silica is known to be a nonadsorbing surface for xanthan molecules.[9] It was chem-mechanically polished down to a rms roughness of less than 3 nm confirmed by Nomarski's interferential contrast measurements. For reasons which will become clear in the following, three sample thicknesses, 50, 100, and 250 μm, were systematically used. The excitation of fluorescence was from an Ar^+ laser ($P = 2$ mW, beam diameter $= 5$ mm, s polarization). The fluorescein emission was detected at 510 nm through a narrow-band interference filter (± 10 nm), with use of a large-aperture collection optics (f-number $= 1$) and photon-counting equipment (Hamamatsu photomultiplier, model R 549). Measurements were controlled by a microcomputer at over 100 different angles, with an angular resolution of 1 mrad. A typical run took about 5 min.

Figure 1 shows the fluorescence intensity $I_F^{\rm pol}$ (on a logarithmic scale) emitted by the 96-ppm xanthan solution versus the angle of incidence θ of the laser beam and for two sample thicknesses, $d = 50$ and 100 μm. We observe two regions separated by a 100-fold increase in I_F, depending on whether θ is higher or lower than θ_c. For $\theta > \theta_c$, the solution fluorescence is excited by the evanescent wave over its shallow penetration length Λ ($\Lambda \ll d$) and the detected intensity is weak. For $\theta < \theta_c$, in contrast, the fluorescence is due to the excitation by the direct transmitted beam. It takes place over the whole sample thickness and is therefore much more intense. This simple picture is, however, too crude to explain the thickness dependence observed in Fig. 1. We must also consider the stray light scattered by the imperfections of the prism surface. They create a volume fluorescence which adds to the true signal and is of course very conspicuous for $\theta > \theta_c$. This spurious contribution increases roughly linearly with d. It can thus be eliminated by performing the experiments at several sample thicknesses and extrapolating to zero d at each incidence angle. On the other hand, the wiggling structure observed below θ_c for the 50-μm-thick sample is due to interferences between the transmitted incident beam and its reflection onto the top surface of the glass cuvette. It induces a set of fringes parallel to the prism surface and therefore an inhomogeneous distribution of light within the sample which changes with the angle of incidence.[17]

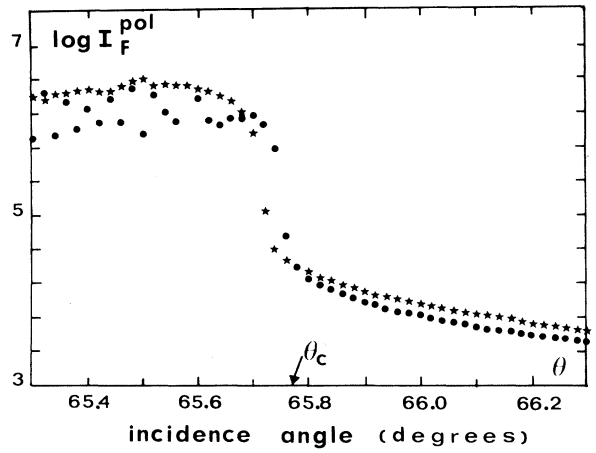

FIG. 1. Fluorescence intensity $I_F^{\rm pol}$ vs the angle of incidence θ for the excitation laser beam. Xanthan polymer concentration $= 96$ ppm (by weight). Sample thicknesses $= 50$ μm (dotted curved) and 100 μm (starred curve).

The above complications can actually be turned into a means for determining the position of θ_c with good accuracy. In the evanescent mode, the dependence on sample thickness should be minimum when Λ is of order d, i.e., for $\theta = \theta_c$. On the other hand, it is easy to show that, in the direct-beam excitation, interference effects appear as soon as $\theta_c - \theta$ is slightly positive (typically $\simeq 10^{-4}$ rad for a 5-mm beam diameter and $d = 50$ μm). Therefore, we have decided to take θ_c as the point where the curves for the two different thicknesses cross each other, i.e., where I_F is the least dependent on d. The data obtained with the third sample thickness, not represented here, also yield the same determination of θ_c. Our angular resolution is 0.02° and allows us to precisely control the beam incidence angle relative to θ_c, which is a crucial point in the data analysis. On the other hand, the absolute value of θ_c is much harder to determine and with our setup cannot be measured to better than 0.1°. Therefore in Fig. 1, we have used the calculated value derived from the well-known refractive indexes n_1 and n_2.

Using this determination of θ_c and the extrapolation procedure to zero sample thickness, we can now plot in Fig. 2 the ratio $R = I_F^{\rm pol}/I_F^{\rm ref}$ as a function of the reciprocal of the penetration length, Λ^{-1}. The

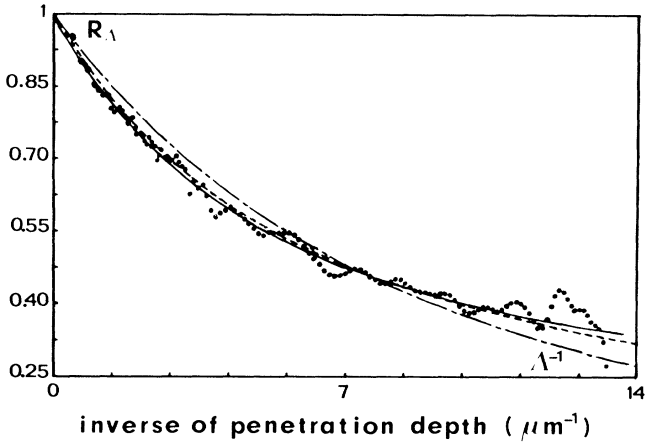

FIG. 2. Fluorescence intensity ratio $R = I_F^{pol}/I_F^{ref}$ vs the inverse of the penetration depth of the evanescent wave, Λ^{-1}. Xanthan polymer concentration =96 ppm. The data have been extrapolated to zero sample thickness (see text). The lines correspond to the best fit with a $\tanh^2$ profile for flexible chains (dot-dashed curve), the Auvray profile for rigid rods (dashed curve), and a mixed "rigid-then-flexible" profile (solid curve).

large decrease in $R(\Lambda)$ with Λ^{-1} gives immediate evidence for the existence of a depletion layer since it means that, as one probes regions closer and closer to the solid wall, the fluorescence intensity of the polymer solution decreases with respect to the intensity emitted by the reference solution with uniform concentration. It is easy to show by differentiation of Eq. (1) that the slope at the origin gives an estimate of the mean depletion-layer thickness $e = \Gamma\Phi_b^{-1}$ where Γ is the surface excess defined by $\Gamma = \int_0^\infty [\Phi(Z) - \Phi_b]dZ$. Indeed, writing $\Phi(Z)$ as $\Phi_b + \Delta\Phi(Z)$ with $\Delta\Phi = \Phi(Z) - \Phi_b$ in Eq. (1), we obtain

$$R(\Lambda) = 1 + \frac{1}{\Phi_b \Lambda}\int_0^\infty \Delta\Phi(Z)\exp(-Z/\Lambda)\,dZ.$$

This yields

$$\left.\frac{dR(\Lambda)}{d\Lambda^{-1}}\right|_{Z=0} = \frac{1}{\Phi_b}\int_0^\infty \Delta\Phi(Z)\,dZ.$$

Development of $R(\Lambda)$ at first order in Λ^{-1} gives

$$R(\Lambda)|_{\Lambda^{-1}\to 0} = 1 + \Gamma/\Phi_b\Lambda. \quad (2)$$

In our particular case we obtain $e = 150 \pm 15$ nm and $\Gamma = -1.4\times10^{-7}$ g m^{-2}. The error bars on e account for sample reproducibility, intensity-data dispersion, and a 0.01° uncertainty in the position of the θ_c value. The complete concentration profile $\Phi(Z)$ can in principle be extracted from the $R(\Lambda)$ curve by performing an inverse Laplace transform of Eq. (1). However, this is not an easy procedure. We have therefore preferred to calculate analytically $R(\Lambda)$ for various concentration profiles and then to make a least-squares fit with the experimental data using e as the floating parameter. We have plotted in Fig. 2 the result obtained for three different models: (i) the mean-field profile $\Phi(Z) = \Phi_b \tanh^2(Z/e)$ predicted for flexible chains in dilute solutions, where $e \simeq R_G$[4]; (ii) the equilibrium profile $\Phi(Z) = \Phi_b(Z/L)[1 - \ln(Z/L)]$ calculated for a dilute gas of rigid rods of length L[8] (in this case $e = L/4$); (iii) the superposition of the two previous models, i.e., a rigid-rod profile for all distances Z less than the Kuhn length $2q$ (i.e., twice the persistence length q) and a flexible chain profile for all larger distances. We thus have two fitting parameters: $L = 2q$ and $e \simeq R_G$.

Examination of Fig. 2 shows clearly that the flexible model does not give satisfactory agreement with the data over the whole range of Λ^{-1}. In contrast quantitative fits can be achieved with the two models which account for the chain rigidity. The fully rigid chain approach yields an equivalent rod length of $L = 600 \pm 10$ nm. This value is in good agreement with the hydrodynamic determinations which give apparent rod lengths between 700 and 1000 nm, depending on the sample origin.[15] The "rigid-then-flexible" model gives a characteristic distance $e = 180$ nm and a persistance length $2q = 160$ nm. The best estimations in bulk dilute solutions on the same batch of xanthan[12] are 178 nm for the radius of gyration and 100 nm for twice the persistence length. The agreement between e and R_G appears to be very good. The fact that our determination for $2q$ seems larger than expected may be due to the fairly high minimum value of the penetration length Λ. This certainly does not allow the accurate investigation of the concentration profile in the range $Z < 2q$. Also, the model used cannot be taken as rigorous since it does not account for a smooth transition between the rod and the flexible-chain profiles in the vicinity of $Z = 2q$. Further work is under way to clarify this point. Despite all these limitations, observation of Fig. 2 shows that this mixed approach nevertheless provides a slightly better fit to the data than the rigid-rod model. Moreover, it is certainly more realistic.

To conclude, the present experiments demonstrate the existence of a depletion layer for solutions of stiff xanthan chains in contact with a nonadsorbing fused silica surface. The negative surface excess is the lowest ever detected. It is interesting to note that the rigidity of the chain must be taken into account in the interpretation of our data. The technique used here is thus sensitive to relatively subtle changes in the monomer concentration profiles between flexible and stiff chains. Good quantitative agreement is obtained with the Auvray model for fully rigid rods, conditional on the use of an equivalent rod length $L = 600 \pm 10$ nm, much shorter than the curvilinear distance $L_c = 1800$

nm. Even better agreement is achieved with the "rigid-then-flexible" model in which the chain-persistance length separates a domain where the chain can be locally considered as a rod from a domain, at larger scales, where the chain is mostly flexible.

This first measurement of an interfacial profile at a solid-liquid boundary should trigger new experiments on adsorption-depeletion layers in binary mixtures and polymer solutions, wetting-dewetting transitions, etc.

We thank J. Lecourtier and G. Chauveteau for numerous discussions on the properties of xanthan in solution and also for the generous gift of fluorescein-labeled xanthan chains. This work has been supported by the Centre National de la Recherche Scientifique under an Action Thematique Programmee "polymères aux interfaces" No. 070542. Physique de la Matièr, Condensée is a Unité Associée au Centre National de la Recherche Scientifique No. 792. One of us (D.A.) has benefitted from a research scholarship from Elf-Aquitaine.

[1]S. Asakura and F. Oosawa, J. Chem. Phys. **22**, 1255 (1954).

[2]R. I. Feigin and D. H. Napper, J. Collod. Interface Sci. **75**, 525 (1980).

[3]E. di Marzio and M. McCrackin, J. Chem. Phys. **43**, 539 (1965).

[4]P. G. de Gennes, L. Leibler, and J. F. Joanny, J. Polym. Sci. Polym. Phys. Ed. **17**, 1973 (1979).

[5]E. F. Casassa, Macromolecules **17**, 601 (1984).

[6]P. G. de Gennes, J. Phys. (Paris) **37**, 1445 (1976), and **38**, 426 (1977).

[7]P. G. de Gennes, Macromolecules **14**, 1637 (1981).

[8]L. Auvray, J. Phys. (Paris) **42**, 79 (1981).

[9]G. Chauveteau, Rheology **26**, 111 (1982); G. Chauveteau, M. Tirrell, and O. Omari, J. Colloid Interface Sci. **100**, 41 (1984).

[10]A. P. Gast, C. K. Hall, and W. B. Russell, J. Colloid Interface Sci. **96**, 251 (1983).

[11]C. Allain, D. Ausserré, and F. Rondelez, Phys. Rev. Lett. **49**, 1694 (1982).

[12]G. Muller, J. Lecourtier, G. Chauveteau, and C. Allain, Makromol. Chem. Rapid Commun. **5**, 203 (1984).

[13]Double helical dimers with a larger persistence length ($q = 120$ nm) and a larger diameter (2.0–2.5 nm) have also been reported recently by T. Sato *et al.*, Polym. J. **16**, 423 (1984). However, the chain chemistry is slightly different in their case.

[14]H. Yamakawa, *Modern Theory of Polymer Solutions* (Harper and Row, New York, 1971).

[15]S. L. Wellington, Polym. Prepr. Am. Chem. Soc. Div. Polym. Chem. **22**, 63 (1981).

[16]H. Hervet, D. Ausserré, and F. Rondelez, in *Physical Optics of Dynamic Phenomena and Progress in Macromolecular Systems,* edited by B. Sedlacek (de Gruyter, New York, to be published). See also Ref. 11.

[17]The wiggling structure is not observed with the 100-μm-thick sample because the spatial region where the two beams interfere shifts away from the detector viewing area for incidence angles between θ_c and $\theta_c + 0.1°$. At larger angles, the interferences could in principle be detected but the fluorescence signal is the result of an integration over a large number of fringes in the cell and its average level is also higher. Both factors reduce the amplitude of the fluctuations for the thicker sample in Fig. 1.